Numerical modeling of fracture processes of bodies with stress concentrators under conditions of proportional loading, taking into consideration the statistical distribution of ultimate strength and partial loss of load bearing capacity

E.V. Feklistova, A.I. Mugatarov, V.E. Wildemann
Center of Experimental Mechanics, Perm National Research Polytechnic University, Russia
cem.feklistova@mail.ru, https://orcid.org/0000-00020025-6204
cem_mugatarov@mail.ru, https://orcid.org/0000-0002-2229-8181
wildemann@pstu.ru, https://orcid.org/0000-0002-6240-4022

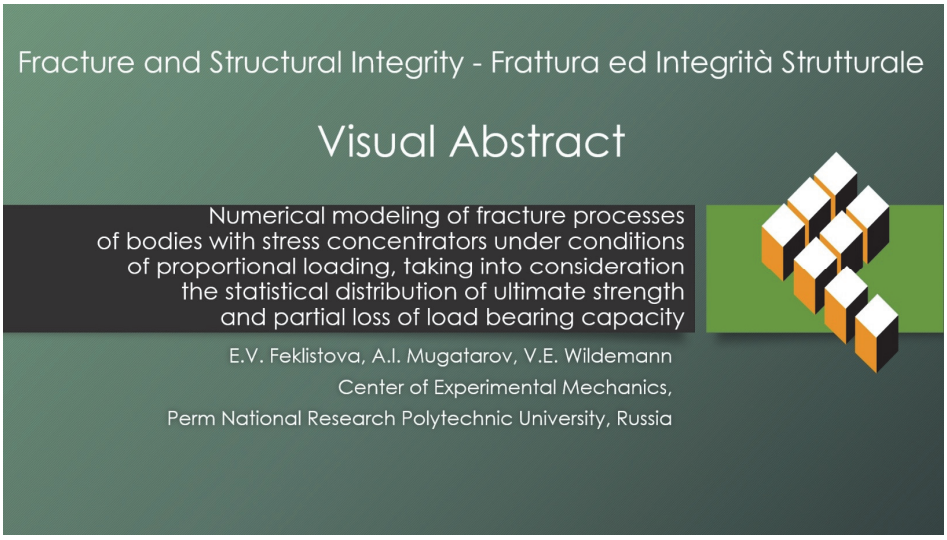

KEYWORDS. Fracture, Finite element method, Numerical modeling, Brittle body, Strength properties distribution.

OPEN ACCESS

Citation: Feklisova, E.V, Mugatarov, A.I., Wildemann, V.E., Numerical modeling of fracture processes of bodies with stress concentrators under conditions of proportional loading, taking into consideration the statistical distribution of ultimate strength and partial loss of load bearing capacity, Fracture and Structural Integrity, 74 (2025) 55-72.

Received: 03.07.2025
Accepted: 28.07.2025
Online first: 29.07.2025
Published: 01.10.2025

INTRODUCTION

Fracture of structures is a complex multi-stage process that occurs at various scale levels: initial micro-fractures are formed in the sample's volume, leading to the appearance of microdefects, which, in turn, form larger damaged zones, leading to the appearance of macrodefects and main cracks [1]. A large number of fundamental works [2, 3] is dedicated to the mathematical description of these processes; many models of the behavior of samples with cracks were proposed: linear elastic model [4], cohesive zone models, continuum damage models, bridged crack models, etc. One of the

simplest, but at the same time actively used approaches is the approach that reduces the stiffness of local areas in which the failure criterion is met [5-8]. A large number of damaged areas leads to the formation of macrodefect and destruction of the structure. The numerical implementation of this approach in the framework of the finite element method requires consideration of many aspects: the organization of numerical procedures, the selection of the loading step size; consideration of the influence of the finite element mesh' size, discussed in detail in [5].

Due to the inhomogeneity of the stress-strain state, local areas of the structure fail at the same time, which makes it necessary to describe the processes of stresses redistribution and possible fracture of the neighboring areas. To identify the type of damage and describe the processes of fracture in the material, various semi-empirical (phenomenological) or structural models of damage accumulation are used, which makes it possible to obtain kinetic equations for assessing the level of fracture [1, 9-14]. Moreover, the use of several failure criteria within the framework of structural-phenomenological models makes it possible to distinguish the mechanisms of structural elements' fracture [1]. For example, Novembre E. et al. [10], within the framework of the concept of two-phase decomposition of the composite (into fibers and matrix), when the Tsai-Wu failure criterion was triggered, carried out the degradation of elastic properties in the plane of the matrix phase through a single scalar damage variable. Airoldi A. et al. [12], within the framework of the similar concept, simulated splitting and transverse cracking in the composite matrix by varying the stiffness properties in the fiber and matrix phases. All types of matrix damage were presented within a single constitutive law attributed to the idealized matrix phase. A polynomial model of damage evolution, which depends on the damage threshold associated with failure energy per unit volume, was used by Pabbu K.M. [13] to model isotropic continuum damage in hyperelastic materials. Rui J. et al. [14] used a structural damage model based on the strain energy of the structure to estimate the overall extent of damage after the earthquake and to provide recommendations for structural reinforcement and repair. It is of interest to further develop structural-phenomenological models describing fracture processes in order to conduct an updated analysis of structures behavior in the conditions of damage accumulation.

In addition, since the physical and mechanical (in particular, strength) properties of the material at different points of the structure are random values that vary in a certain range, consideration of the statistical spread of properties when performing refined strength calculations, taking into account local fracture, will make it possible to predict the reliability, survivability and bearing capacity of the structure more accurately [15-17]. It is noted that not only the heterogeneity of the distribution of structural elements' mechanical properties over the body's volume, but also the type of the distribution law, have a significant impact on the results of fracture processes modeling [5-8, 16, 18].

It is known that the local concentration of stresses in the deformed body leads to the implementation of inhomogeneous stress and strain fields, and causes damage to the structure during operation [19]. Since the presence of a stress concentrator significantly changes the strength of the entire structure, lots of work is dedicated to the study of structures' strength in the presence of stress concentrators under axial tensile and biaxial loadings [8, 19-25]. In particular, the authors [8] considered the effect of the elliptical stress concentrator's geometry on the process of fracture at various values of the standard deviation of the distribution of finite elements' ultimate strength. Khechai A. and Mohite P. [19] conducted analytical studies to determine the optimal values of the effective parameters of the stress concentration coefficient around the cutout in orthotropic plates under uniaxial and biaxial loadings. In the work [20], for a plate with a circular concentrator, a decrease in the stress concentration coefficient from 3 at uniaxial tension to 2.1 for a plate loaded biaxially was revealed. By the team of researchers Jagannathan N. et al. [21] matrix cracking was simulated in polymer matrix composites for various biaxial loading options; Weibull distribution was used to account changes in the transverse strength of the layer. It was noted that statistical strength methods can better predict crack propagation, compared to strain energy estimation approaches. Mechanical properties and fracture behavior of the cracked sandstone disks were studied at various axial and lateral load ratios by Ma C. et. al. [25]. It was found that both the peak load and the initial load decreased with the increase of the initial crack's angles and the ratio of axial and lateral loads, with the fracture pattern of the discs changing from shear failure to a combination of tensile and shear failure and, finally, to pure tensile failure. It is possible to draw a conclusion about the significant effect of multi-axis loading of bodies with stress concentrators on the processes of structural failure.

This work is dedicated to the development of a fracture model of elastic-brittle material with statistically distributed strength characteristics of subregions, as well as to the application of this model for description of the fracture processes of the bodies with stress concentrators under biaxial loading. The "Methodology" section presents the main results and disadvantages of the previous works [5-8], and describes the methodology of this work. The section "Boundary value problem and its solution algorithm" provides an improved statement of the problem, presents a model of the material with the occurrence of anisotropy during partial fracture, and also presents an algorithm for solving this boundary value problem. The section "Results and discussion" presents and analyzes the results of fracture process modeling of a plate with a round stress concentrator under biaxial loading, as well as the results of applying previously developed approach for assessment of the type of damage accumulation based on solving boundary value problems of the theory of elasticity. In the "Conclusions" section, the main conclusions on the work are given and possible directions for further research are indicated.

METHODOLOGY

Previously, the authors carried out the numerical study of the destruction processes of bodies with stress concentrators, considering the elastic-brittle material with various strength properties of structural elements [6-8]. The main findings of the previous research were:

1. Consideration of the failure processes, taking into account the heterogeneity of the distribution of strength properties of structural elements, during which variating structure's macrolevel behavior takes place (from elastic-brittle to quasi-plastic with realization of the postcritical stage) depending on the value of the ultimate strength dispersion;
2. Three characteristic types of damage accumulation were identified: localized (with the development of a macrodefect), dispersed (with the accumulation of damage in the entire volume), mixed (with the growth of a macrodefect in the most weakened areas). To assess the type of damage accumulation, based on the results of solving boundary value problems of the theory of elasticity, a new approach has been proposed, which consists in the analysis of overload coefficients;
3. The geometry of the stress concentrator has a significant impact on the behavior of the structure at the macro level and the strength reserve, however, there is a threshold value of the variation coefficient of ultimate strength, after which the concentrator ceases to affect the behavior of the structure;
4. Reducing the size of the finite elements leads to a decrease in the load bearing capacity of the body, while there is no convergence of the numerical solution. In this regard, it is suggested that the characteristic size of finite elements should be physically justified and selected for different materials on the basis of experimental studies.

Nevertheless, several disadvantages and limitations were noted:

1. The works consider only a uniform distribution, poorly suitable for describing a random distribution of material's mechanical properties, and a two-parameter Weibull distribution, using which close to zero values of ultimate strength were generated;
2. In the work, at the realization of the fracture criterion, all stiffness properties of the final element were reduced, which does not quite correspond to the real behavior of elastic-brittle materials, for which the bearing capacity disappears, when stretched across the crack plane, and remains, when deformed along the crack plane (i.e. significant anisotropy of properties appears). This drawback can be significant when modeling fracture processes under biaxial loading conditions;
3. Only uniaxial loading was considered.

The methodology of the study was improved in the following way, taking into account the mentioned disadvantages:

1. *Material.* Elastic-brittle material without plastic deformation, viscoelastic behavior or friction between damaged parts of the structure is considered. The body is divided into subregions, the material inside each subregion is isotropic and homogeneous, the elastic moduli at all points are the same, the ultimate strength is distributed statistically according to the three-parameter Weibull law. Partial loss of the bearing capacity of the material within the subregion occurs when the first principal stress reaches ultimate strength. In this case, in the subregion, the intact isotropic material is replaced by an orthotropic one, the anisotropy axes of which are oriented in accordance with the directions of the principal stresses at the moment of damage (the propagation of the crack through the subregion is simulated). Elastic properties of the orthotropic material ensure absence of resistance during the deformation across the simulated crack, but show resistance during the deformation along it. In case, when in the material, that has partially lost its bearing capacity, the normal stress (oriented along the simulated crack) again exceeds the ultimate strength, the material is replaced with an isotropic one that has completely lost its bearing capacity. Since the material that has completely lost its bearing capacity is extremely malleable, geometric nonlinearity is considered. The described scheme for the material properties' changing, when the failure criterion is met, is illustrated in Fig. 1. The implementation of this scheme is described in the section "Boundary value problem and its solution algorithm".
2. *Body with stress concentrator at biaxial loading.* A body with an internal stress concentrator in a plane stress state (plate) is considered. Kinematic boundary conditions are applied to the outer boundaries of the body, while changes of all displacements are made proportionally (i.e. complex loading is not considered). At the boundaries of the stress concentrator, boundary conditions of the second type with zero forces are applied;
3. *Features of the numerical realization.* When dividing a body into finite elements, it is assumed that one subregion (within which the material is homogeneous) corresponds to one finite element. Also, there is no additional consideration of the effect of the size of the finite element mesh on the modeling results, it is initially built small. These assumptions help to avoid the necessity of building a random structure of the material inside the body and reduce the number of tasks to be solved, while ensuring the possibility of checking the adequacy and feasibility of the developed model's applicability. In accordance with the results of work [5], at each stage of solving the boundary value problem, one of the most overloaded elements is deactivated, the loading step is selected automatically, based on the analysis of stress fields, in case of damage or

deactivation of one finite element, the boundary conditions remain unchanged until a stable state is obtained. For each of the variation coefficients, five generations of finite elements' ultimate strength will be considered, for each of the generations, different modes of multiaxial loading will be implemented;

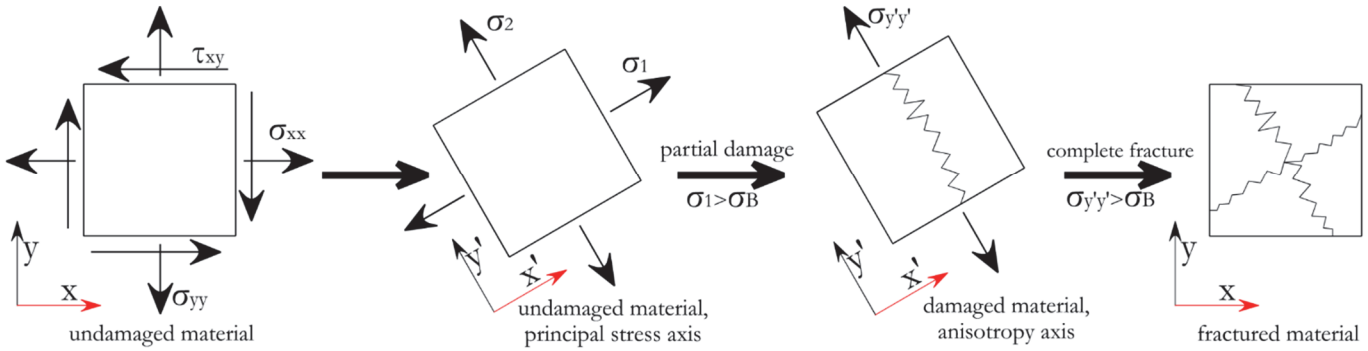

Figure 1: The scheme of the material properties reduction after the fracture criterion fulfillment (plane stress state): x, y are global coordinate system axes; x', y' are the anisotropy axes of the damaged material, corresponding to the orientation of the principal stress before damage.

4. *Registered data and their analysis.* After each of the calculations, data on the displacements of the external boundaries of the body and the emerging reaction forces are registered, which allows building diagrams of the body's load at the macro level. The number of each damaged/deactivated element is also registered, which allows analyzing the kinetics of the fracture process and assessing the integral damage to the body structure;
5. *Assessment of the type of damage accumulation.* In accordance with the approach proposed in [7], for the obtained generations of ultimate strength of structural elements, an analysis of overload factors during the elastic deformation of the body will be carried out with an estimation of the number of FEs, in which the threshold value is exceeded, and estimation of the average distance from the concentrator to centers of these FEs. The plotted dependences of these values on the variation coefficient of the ultimate strength will be associated with the realization of the previously identified types of damage accumulation.

Based on the application of the developed methodology, conclusions will be drawn about the adequacy and feasibility of the developed model's applicability.

BOUNDARY VALUE PROBLEM AND ITS SOLUTION ALGORITHM

Mathematical formulation

The solid is represented as a set of N subregions, whose ultimate strength is defined by using the indicator function:

$$\chi^{(z)}(\overline{r}) = \begin{cases} 1, \overline{r} \in V^{(z)} \\ 0, \overline{r} \notin V^{(z)} \end{cases}$$
$$\sigma_B(\overline{r}) = \sum_{z=1}^{N} \sigma_B^{(z)} \chi^{(z)}(\overline{r}) \quad (1)$$

Here $\overline{r}$ is the radius vector; $\chi^{(z)}$ is the indicator function, characterizing the point location in the subregion indexed (z) with the volume $V^{(z)}$; V is the entire body volume; σ_B is the piecewise-constant function that specifies the ultimate strength values distribution over the solid; $\sigma_B^{(z)}$ is the ultimate strength value in the subregion indexed (z).

In order to take the history of the damaging process into account, the parameter t (a conditional analogue of time) is introduced into the problem. Thus, displacement vector and tensors of strain, stress and elastic properties depend on the process parameter. Since each subregion is elastic-brittle, the assumption is made that the destruction of subregion occurs when the maximum value of the first principal stress σ_1 in the subregion's volume reaches the ultimate strength value. To compare the failure risk in various points of the solid, the overload factor K is considered:

$$K(\bar{r},t)=\frac{\sigma_1(\bar{r},t)}{\sigma_B(\bar{r})} \tag{2}$$

Since the strains in the damaged subregions can be much greater than in undamaged ones, the using of the Lagrangian strain tensor is preferrable. On the other hand, it is supposed that the deformation of the subregion does not lead to a significant change of its shape, size and configuration, so the Cauchy stress tensor can be used instead of Piola–Kirchhoff stress tensor. The equations of equilibrium (no mass forces are considered), the strain-displacement equations and the constitutive law (using generalized Hooke's law, taking into account the scheme of material properties alternation after damage) are represented as:

$$\sigma_{ij,j}(\bar{r},t)=0$$

$$\varepsilon_{ij}(\bar{r},t)=\frac{1}{2}\left(u_{i,j}(\bar{r},t)+u_{j,i}(\bar{r},t)+u_{k,i}(\bar{r},t)u_{k,j}(\bar{r},t)\right)$$

$$\sigma_{ij}(\bar{r},t)=C_{ijkl}(\bar{r},t)\varepsilon_{kl}(\bar{r},t)$$

$$C_{ijkl}(\bar{r},t)=\sum_{\tilde{z}=1}^{N}C_{ijkl}^{(\tilde{z})}(t)\chi^{(\tilde{z})}(\bar{r});$$

$$C_{ijkl}^{(\tilde{z})}(t)=\begin{cases} C_{ijkl}^{init}, \nexists\tau\le t:\max\limits_{V^{(\tilde{z})}}\left(K(\bar{r},\tau)\right)\ge 1 \\ \alpha_{im}^{(\tilde{z})}\alpha_{jn}^{(\tilde{z})}\alpha_{kp}^{(\tilde{z})}\alpha_{lq}^{(\tilde{z})}C_{mnpq}^{dam}, \exists\tau\le t:\max\limits_{V^{(\tilde{z})}}\left(K(\bar{r},\tau)\right)\ge 1\wedge\forall\tau'<\tau:C_{ijkl}^{(\tilde{z})}(\tau')=C_{ijkl}^{init} \\ C_{ijkl}^{fract}, \exists\tau\le t:\max\limits_{V^{(\tilde{z})}}\left(K(\bar{r},\tau)\right)\ge 1\wedge\exists\tau'<\tau:C_{ijkl}^{(\tilde{z})}(\tau')=C_{ijkl}^{dam} \end{cases}$$

$$C_{ijkl}^{init}=\lambda\delta_{ij}\delta_{kl}+G\left(\delta_{ik}\delta_{jl}+\delta_{il}\delta_{jk}\right),\lambda=\frac{\nu E}{(1+\nu)(1-2\nu)},G=\frac{E}{2(1+\nu)}$$

$$C_{mnpq}^{dam}=C_{mnpq}^{init},\ \text{but}\ C_{1111}^{dam}=C_{1122}^{dam}=C_{1133}^{dam}=C_{1313}^{dam}=C_{1212}^{dam}=0$$

$$\alpha_{im}^{(\tilde{z})}=\begin{pmatrix} \cos\left(x_1,x_1^{(\tilde{z})}\right) & \cos\left(x_1,x_2^{(\tilde{z})}\right) & \cos\left(x_1,x_3^{(\tilde{z})}\right) \\ \cos\left(x_2,x_1^{(\tilde{z})}\right) & \cos\left(x_2,x_2^{(\tilde{z})}\right) & \cos\left(x_2,x_3^{(\tilde{z})}\right) \\ \cos\left(x_3,x_1^{(\tilde{z})}\right) & \cos\left(x_3,x_2^{(\tilde{z})}\right) & \cos\left(x_3,x_3^{(\tilde{z})}\right) \end{pmatrix} \tag{3}$$

$$C_{ijkl}^{fract}\equiv 0$$

Here σ_{ij} is the stress tensor; ε_{ij} is the Lagrangian strain tensor; u_i is the displacement vector; C_{ijkl} is the elastic constants tensor represented as piecewise-constant function that specifies the elastic properties $C_{ijkl}^{(\tilde{z})}$ of the subregion indexed ($\tilde{z}$); C_{ijkl}^{init} is the elastic properties tensor of the undamaged (initial) material; E, ν, λ, G are the elastic constants of the isotropic material: Young's modulus, Poisson's ratio, Lamé moduli, respectively; δ_{ij} is the Kronecker delta; C_{ijkl}^{dam} is the elastic properties tensor of the damaged material with partial bearing capacity loss (i.e. the failure criterion was implemented once), the elastic properties are reduced in direction $x_1^{(\tilde{z})}$; (x_1, x_2, x_3) is the global coordinate system; ($x_1^{(\tilde{z})}$, $x_2^{(\tilde{z})}$, $x_3^{(\tilde{z})}$) is the local coordinate system of the orthotropic damaged material in the subregion indexed ($\tilde{z}$), associated with the direction of the principal stresses at the moment of partial bearing capacity loss (similar to the global coordinate system for the undamaged material); $\alpha_{im}^{(\tilde{z})}$ is the rotation matrix from the local coordinate system to the global one; C_{ijkl}^{fract} is the elastic properties tensor of material after complete bearing capacity loss.

The problem is supplemented by the displacement boundary conditions and the traction boundary conditions:

$$\begin{cases} u_i(\bar{r},t)\big|_{\Gamma_u} = u_i^0(\bar{r},t) \\ \sigma_{ij}(\bar{r},t)n_j(\bar{r})\big|_{\Gamma_S} = S_i^0(\bar{r},t) \end{cases} \quad (4)$$

Here u_i^0 is the displacement vector applied to the boundary Γ_u; S_i^0 is the stress vector applied to the boundary Γ_S; n_j is the unit normal vector to the boundary Γ_S. The Eqns. (1)–(4) form the boundary value problem of deformation and fracture of the solid body, taking into account inhomogeneity of strength properties and partial loss of bearing capacity of material.

Solution algorithm

For the numerical solution of the boundary value problem with the improved research methodology given in the previous section, the previous algorithm, which feasibility was proven in [5–6], is modified to take into account the change in material properties due to damage. The modified algorithm for solving the boundary value problem includes:

1. Initial data input: elastic properties 1 – undamaged isotropic material; elastic properties 2 – damaged orthotropic material, for which it is necessary to take into account the rotation of the anisotropy axes in the direction of the principal stresses at the moment of damage; elastic properties 3 – fractured isotropic material. Generating of the ultimate strength values of FE according to the chosen probability distribution law.
2. Creation output files Φ_1 and Φ_2 with the solution results.
3. Designing and meshing of the body.
4. Creating of the initial boundary conditions (Eq. (4)), u_i^0 and S_i^0 values should be small to prevent the failure criterion fulfillment at the first step.
5. Calculating of the stress-strain state.
6. Calculating of the external load value $P_{(i)}$ (if the loading is multiaxial, several values are calculated). Here (i) is the step number. Output to Φ_1: (i), $u_{(i)}$, $P_{(i)}$.
7. If $P_{(i)}$ value is less than the critical value P_{crit}, the fracture modeling process ends (except for the first step) and the resulting data files Φ_1, Φ_2 are saved.
8. Calculating of the field of the overload coefficient K (Eq. (2)), defining of its maximum value K_{max} and the number (m) of the element with K_{max}.

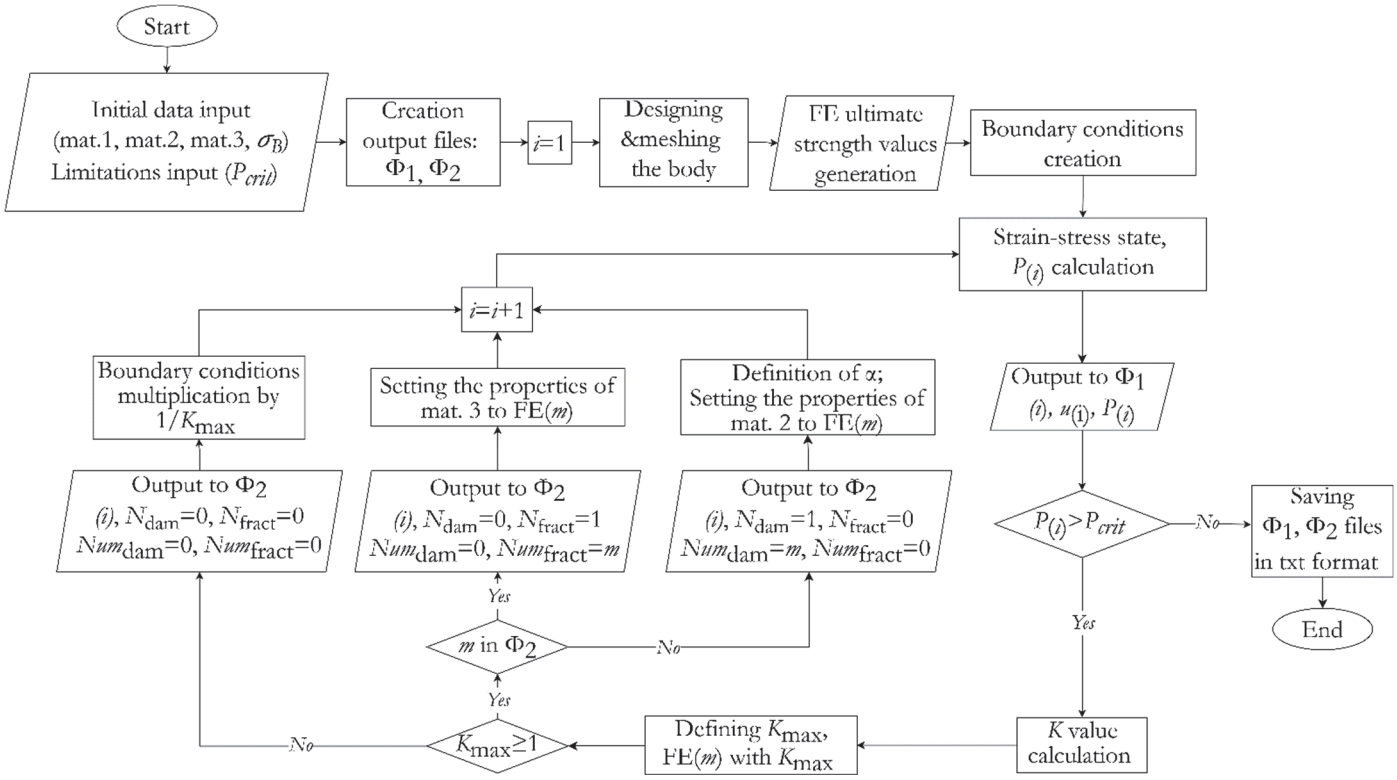

Figure 2: The flow chart of the boundary value problem solution algorithm.

9. If $K_{max}\geq 1$ and the finite element with number (m) is assigned the properties of the material with elastic characteristics 1, then the angle of rotation of the local coordinate system relative to the global one is determined in accordance with the directions of the principal stresses and the elastic properties of an orthotropic material 2 are assigned, $N_{dam}=1$, $N_{fract}=0$, $Num_{dam}=m$, $Num_{fract}=0$. If $K_{max}\geq 1$ and the finite element with number (m) is assigned the properties of a material with elastic characteristics 2, then it is assigned the elastic properties of material 3, $N_{dam}=0$, $N_{fract}=1$, $Num_{dam}=0$, $Num_{fract}=m$. If $K_{max}<1$, then $N_{dam}=0$, $N_{fract}=0$, $Num_{dam}=0$, $Num_{fract}=0$, magnifying of the boundary conditions $1/K_{max}$ times.
10. Output to Φ_2: (i), N_{dam}, N_{fract}, Num_{dam}, Num_{fract}. Going to the step 5.

The flow chart of the boundary value problem solution algorithm is presented on Fig. 2. As a result of modeling using the data from file Φ_1, the calculated loading diagrams in the load-displacement axes are constructed, and using the data from file Φ_2, images of the body in the current state are output for analyzing the kinetics of the destruction process.

In this work, the ANSYS software package is used. The choice of this package is justified by the possibility of using the built-in procedure for deactivating finite elements "*death of finite element*" to simulate crack growth in solids, as well as the possibility of using the structured scripting language Ansys Parametric Design Language (APDL) to interact with the Ansys Mechanical solver.

Model setup

To study the feasibility of modeling the processes of destruction of elastic-brittle bodies within the framework of the developed methodology, the problem of biaxial kinematic loading of a plate is considered (100 mm wide, 100 mm height and 1 mm thick, plane stress state) with the circular hole stress concentrator (20 mm diameter). The boundary conditions are:

$$\begin{cases} u_y(\bar{r},t)\big|_{\Gamma_1}=0 \\ u_x(\bar{r},t)\big|_{\Gamma_2}=0 \\ u_y(\bar{r},t)\big|_{\Gamma_3}=U_y(t) \\ u_x(\bar{r},t)\big|_{\Gamma_4}=U_x(t) \\ \sigma_{ij}(\bar{r},t)n_j(\bar{r})\big|_{\Gamma_5}=0 \end{cases} \tag{5}$$

The geometry of the body, coordinate system and boundary conditions are shown in Fig. 3a. Five types of loading modes are considered: A, E – uniaxial tension along the x and y axes, respectively; C – proportional tension with U_x equal to U_y; B, D – proportional tension with a twofold difference between the displacements (Fig. 3b).

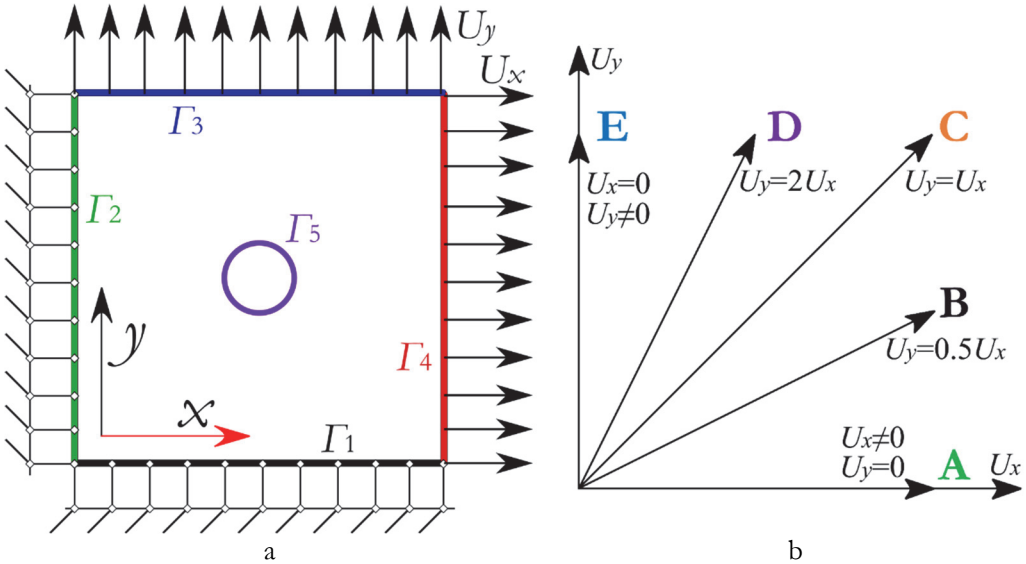

Figure 3: The geometry of the plate and the boundary conditions (a); the proportional biaxial loading modes (b).

A model isotropic material with Young's modulus E=3 GPa and Poisson's ratio ν=0.36 is considered (these properties correspond to the characteristics of the acrylic glass [7]). The ultimate strength values is generated using the three-parameter Weibull distribution:

$$F(\sigma_B)=1-\mathrm{e}^{-\left(\frac{\sigma_B-\sigma_B^{\min}}{\lambda}\right)^{\kappa}};\bar{\sigma}_B=\lambda\Gamma\left(\frac{1+\kappa}{\kappa}\right)+\sigma_B^{\min}$$
$$SD=\lambda\sqrt{\Gamma\left(\frac{2+\kappa}{\kappa}\right)-\left(\Gamma\left(\frac{1+\kappa}{\kappa}\right)\right)^2};CV=\frac{SD}{\bar{\sigma}_B} \quad (6)$$

Here $F(\sigma_B)$ – cumulative distribution function ($\sigma_B \geq \sigma_B^{\min}$); $\sigma_B^{\min}$ – minimum value of tensile strength (chosen equal to $0.1\sigma_B^{\mathrm{mean}}$, where σ_B^{mean}=40 MPa); $\Gamma()$ – gamma function; $\bar{\sigma}_B$ – mean value; SD – standard deviation; CV – coefficient of variation. The distribution parameters κ and λ are selected numerically in a way that $\bar{\sigma}_B$ corresponds to σ_B^{mean}, CV corresponds to the selected value (varied in the range from 0 to 0.5 with a step of 0.1).

In order to discretize the body, the PLANE182 element (with the linear approximation of the displacements field) is used, the mesh is generated automatically in ANSYS. Solving the convergence problem demonstrated that it is sufficient to use the FE with the characteristic linear size of L_{el} =0.33 mm (defined as the square root of the ratio of the body area to the number of FEs), which corresponds to the number of elements N=88656. The critical value of external load P_{crit} is selected equal to 0.1 kN. For a more detailed damaging process consideration, the parameters ω_{dam} and ω_{fract} are introduced, defining the relative number of elements with partially lost bearing capacity (damaged) and completely fractured, respectively.

Numerical experiments were carried out using the high-performance computing complex of the Center for Collective Use "Center of High-Performance Computing Systems" of the Perm National Research Polytechnic University. The results of the fracture process modeling are presented below.

RESULTS AND DISCUSSION

Analysis of feasibility of consideration of bearing capacity partial loss during damage

Demonstration of the realization of anisotropy with a partial loss of bearing capacity. Fig. 4a shows body's part near the stress concentrator, the damaged elements are highlighted in gray, the finite elements that have completely lost their bearing capacity are highlighted in blue. For each of the damaged/deactivated elements, anisotropy axes are shown corresponding to the directions of the first principal stresses at the time of damage: in red for the direction of the first principal stress along which the bearing capacity disappears, in black for the direction of the second principal stress along which the bearing capacity is maintained (corresponds to the direction of the simulated crack that passed through the structural element). The results demonstrate that the orientation of the anisotropy axes corresponds to the direction of macrodefect's growth from the stress concentrator (Fig. 4b).

Comparison of the results of numerical modeling obtained by considering the anisotropy arising from a partial loss of bearing capacity (i.e. using a modified algorithm) with the results obtained by reducing all the stiffness properties of the finite element (previous algorithm [7-8]). The comparison was carried out by using the example of biaxial tension of the plate according to the loading mode C with the variation coefficient CV=0.5; the finite element mesh and the generated distribution of strength properties among finite elements were the same. Fig. 5 shows calculating loading diagrams in the form of dependence of axial loads P_x and P_y on displacements U_x and U_y (for the selected mode U_x=U_y); dependence of the relative amount of damaged and deactivated elements on displacement, as well as images of bodies in states with equal displacements (1 and 1') and equal loads (2 and 2'). The results demonstrate that consideration of the partial loss of bearing capacity led to a significant distortion of the loading diagrams with the implementation of a longer stage of postcritical deformation (when calculating with a complete reduction of mechanical properties, a loss of stability of the numerical solution was observed). It is noted that a sharp drop in load when using a modified algorithm does not lead to an abrupt drop in load along the second loading axis in all cases, since in this direction, when damaged, the bearing capacity remains. It was revealed that diagrams showing increase in the number of damaged and deactivated elements remain similar despite the differences in loading diagrams. The use of the modified algorithm led to a change in the macrodefect growth trajectory, while the areas with 1-3 deactivated elements remained practically unchanged. Total failure, following partial loss of bearing capacity, mainly occurred in the finite elements forming the macrodefect.

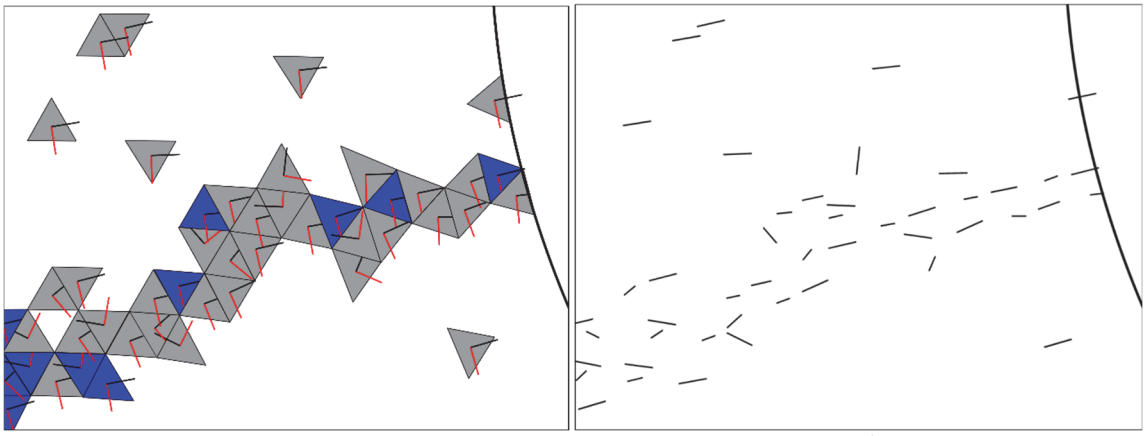

a b

Figure 4: Image of the body with damaged (grey color) and fractured (blue color) FEs, red and black segments represent the orientation of the anisotropy axes of the damaged material (a); image of the imitated cracks (anisotropy axes, along which material properties are unchanged), went through the FEs (b).

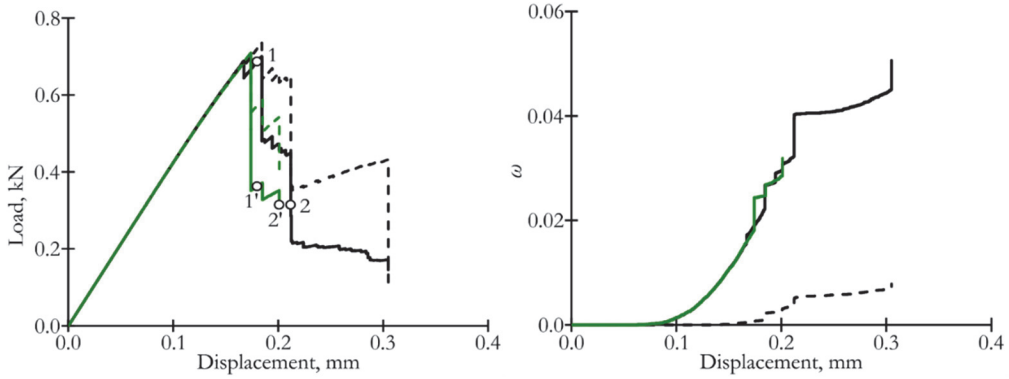

a b

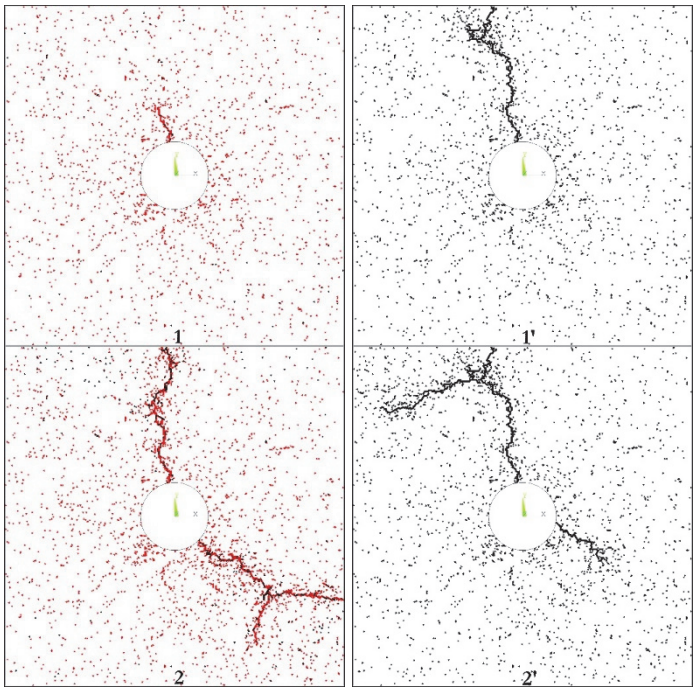

c

Figure 5: The calculated loading diagrams (a), solid plots – $P_x(U_x)$, dashed plots – $P_y(U_y)$; the corresponding diagrams of growth of the relative number of elements with damaged (solid line) and fractured (dashed lines) material (b): black plots – with partial bearing capacity loss taken into account, green plots – without it; the images of the plate with damaged (red color) and completely fractured (black color) elements (c).

On the basis of the obtained results, it is possible to conclude about the operability of the considered model, since in the damaged elements forming the macrodefect, the orientation of the anisotropy axes corresponds to the direction of this macrodefect. Complete failure of elements is possible, and occurs when the failure criterion in the already damaged element is met (for example, at the edges of a growing macrodefect, at the sufficiently low value of the ultimate strength). Since the proposed model of material behavior is more physical, it can be assumed that the results of numerical modeling of fracture processes obtained by using a modified algorithm have greater predictive capability, compared to the results obtained during the complete failure of the finite element. It is important to note that the modified approach is more appropriate for cases of multiaxial loading, since, with uniaxial tension, the effect of maintaining resistance across the direction of load application is practically not manifested in the body's behavior at the macro level. Further improvement of the developed model may be associated with consideration of different resistance under tensile and compressive loadings, which must be studied in cases of complex loading (with a disproportionate change in boundary conditions).
The results of numerical modeling of fracture processes at various coefficients of distribution variation of finite elements' strength properties and loading modes, using the modified model, are presented and analyzed further.

Influence of the coefficient of variation of the ultimate strength distribution on the fracture processes under biaxial loading

Influence of loading mode and variation coefficient of strength properties on the loading diagrams has been considered. Typical loading diagrams are given in Tab. 1. The results demonstrate that an increase in the variation coefficient in all cases leads to a gradual decrease in the bearing capacity of the body and decrease in displacement corresponding to the point of the maximum load, while at the macro level a non-linear deformation begins to appear with the realization of the postcritical stage of body's deformation. However, due to the absence of elements with low strength (as, for example, in the two-parameter Weibull distribution), the loading diagrams are practically linear until the maximum load is reached, pseudoplastic behavior is not observed, unlike in the work [7]. The occurrence of situations, in which a gradual drop in the load on one of the axes leads to a smooth increase in the load on the other of the axes, due to the preservation of resistance in the direction transverse to the direction of macrodefect's growth, was noted. Changing the loading mode with equal variation coefficients of strength properties distribution did not qualitatively affect the type of loading diagrams, however, a non-monotonic change in the maximum loads along the x and y axes sustained by the body was observed. In all loading modes, maximum forces P_x and P_y were achieved simultaneously.

Type of loading	$P_x(U_x)$	$P_y(U_y)$
A/E	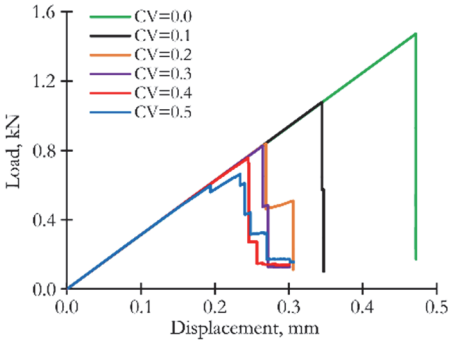	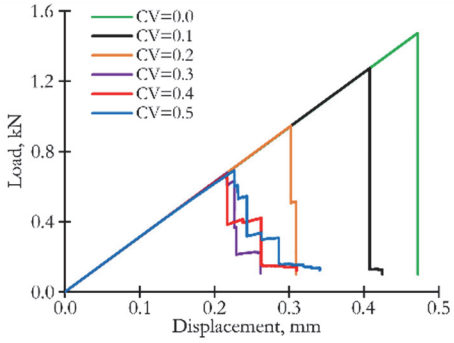
B	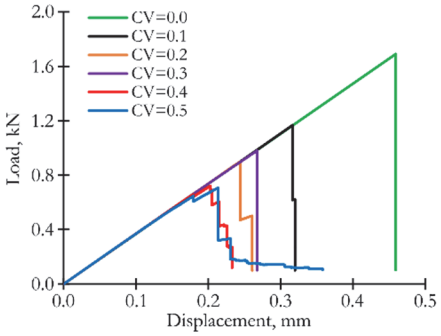	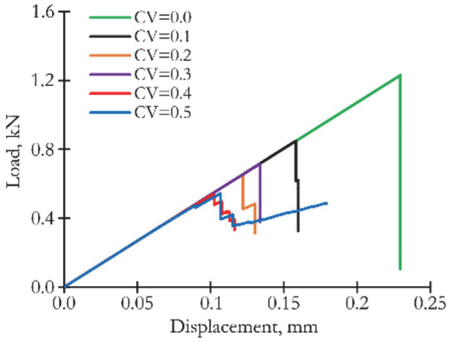

C	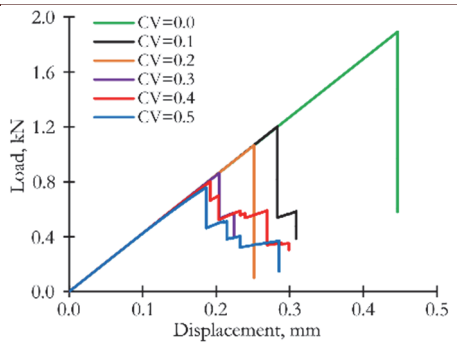	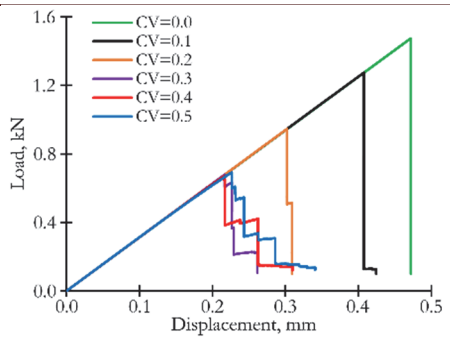
D	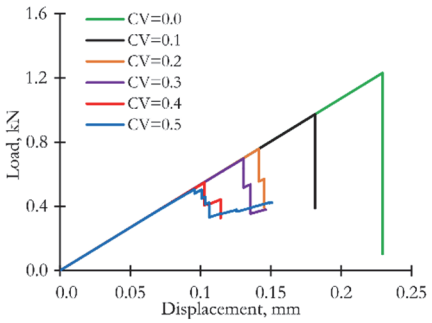	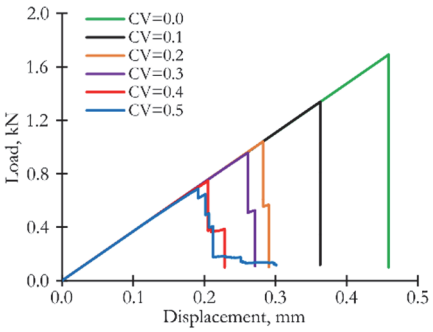

Table 1: The calculated loading diagrams for the various loading modes and coefficients of variation of strength properties.

Fig. 6 shows the strength surface for a body with a stress concentrator under biaxial kinematic loading. The points indicate the values of the maximum load along the x and y axes, averaged according to five calculations. The results demonstrate that a decrease in the coefficient of variation of strength properties distribution leads to an almost linear drop in the maximum load, therefore, it is possible to estimate the bearing capacity of the body at intermediate values of the variation coefficients. It is noted that at high CV values (0.4 and 0.5), the maximum load changes slightly and stays within the statistical error. At the same time, it was indicated that as the load mode A transitions to mode E, a non-monotonic change in the maximum force value P_x occurs: smooth growth (practically unchanged at $CV \geq 0.3$), then a sharp decline; change in P_y occurs as well: a sharp rise, then a smooth decline (almost unchanged at $CV \geq 0.3$). The maximum bearing capacity of the body is achieved under biaxial loading with U_x equal to U_y. The strength surface for the body is practically symmetric in relation to the line $P_y=P_x$, since a sufficiently small finite element mesh is used and the body is symmetrical to the diagonal.

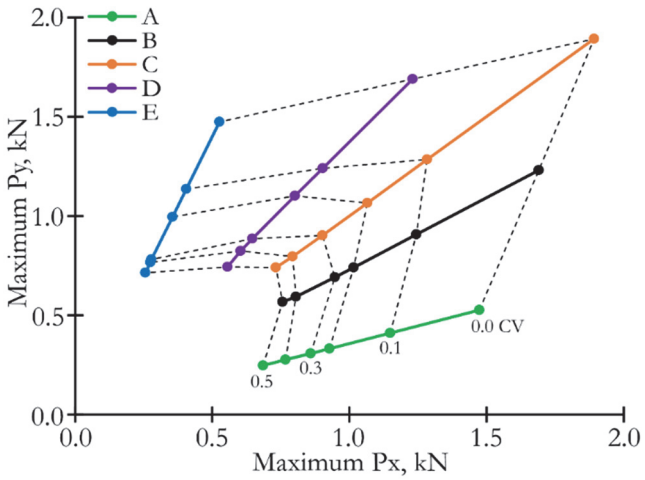

Figure 6: The strength surface of the plate with the stress concentrator.

The evolution of the fracture process has been studied in detail. Fig. 7 shows the calculated loading diagrams, the relationship between the two forces P_x and P_y, diagrams of growth of the number of damaged and completely deactivated elements, as well as the fields of the first principal stresses at some points for the plate with CV=0.2 under loading mode C. It has been

indicated that upon reaching the maximum load (state 1) there is a small number of dispersed deactivated elements in the body (due to the low values of ultimate strength in them). It was noted that despite the elastic-brittle behavior at the macro level and the almost coinciding $P_x(U_x)$ and $P_y(U_y)$ dependences, there is a disproportionate drop in loads during the fracture process, which is associated with asymmetric (relative to the diagonal of the body contour) propagation of the macrodefect at an angle, first in one (state 2), then in the other part of the sample (state 3). At the same time, dispersed deactivated elements have practically no effect on the direction of macrodefect growth due to their small number; a localized type of damage accumulation is realized almost in its pure form. Diagrams of the relative number of damaged and deactivated elements have a sharp rise in value at displacement, which corresponds to reaching the maximum load, which is characteristic for the elastic-brittle behavior of the body at the macro level.

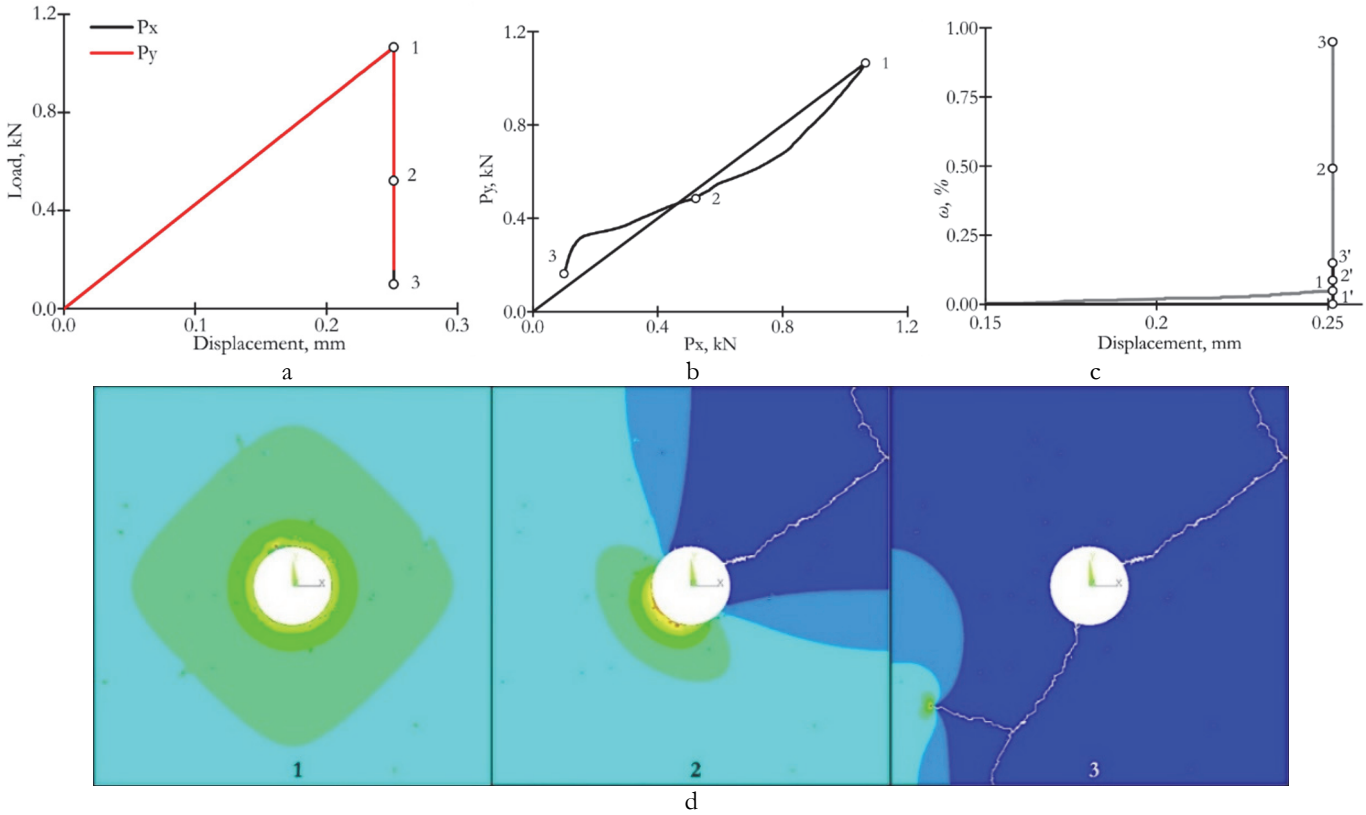

Figure 7: The calculated loading diagrams, states 1–3 are shown on the dependence $P_y(U_y)$ (a), the dependence of P_y on P_x (b), the diagrams of the growth of the relative number of damaged (gray line) and completely fractured (black line) elements (c), the kinetics of the damaging process (d) for CV=0.2 under proportional loading with $U_x=U_y$.

Fig. 8 shows similar results for the loading of the plate with CV=0.5 under the loading mode C. It can be noted that the increase in the variation coefficient of the strength properties led to a significant difference between the loading diagrams $P_x(U_x)$ and $P_y(U_y)$, as well as to the manifestation of a significant disproportionality between the forces P_x and P_y; the unloading trajectory has a complex appearance with local growth areas of one of the efforts. It was revealed that even before reaching the maximum load, multiple dispersed accumulation of damage occurs (state 1) with the formation of a small crack at the concentrator (states 2, 3). The primary crack propagated along the y axis (state 4), which is explained by the uniform distribution of the first principal stresses along the contour of the round concentrator at $U_x=U_y$ (in such conditions, the crack can grow in any direction). Until state 4, there were almost no elements with a material that had completely lost its bearing capacity. A further sharp drop in loads along both axes occurred as the macrodefect, oriented at an angle (states 5, 6), propagated. Complete deactivation of the body occurred after propagation of the macrodefect, oriented along the x axis (states 7, 8), while the failure was accompanied by an intensive decrease in P_y load with almost unchanged P_x load. For a body with CV=0.5, a mixed type of damage accumulation is characteristic, in which the growth of macrodefects occurs over the local damaged areas.

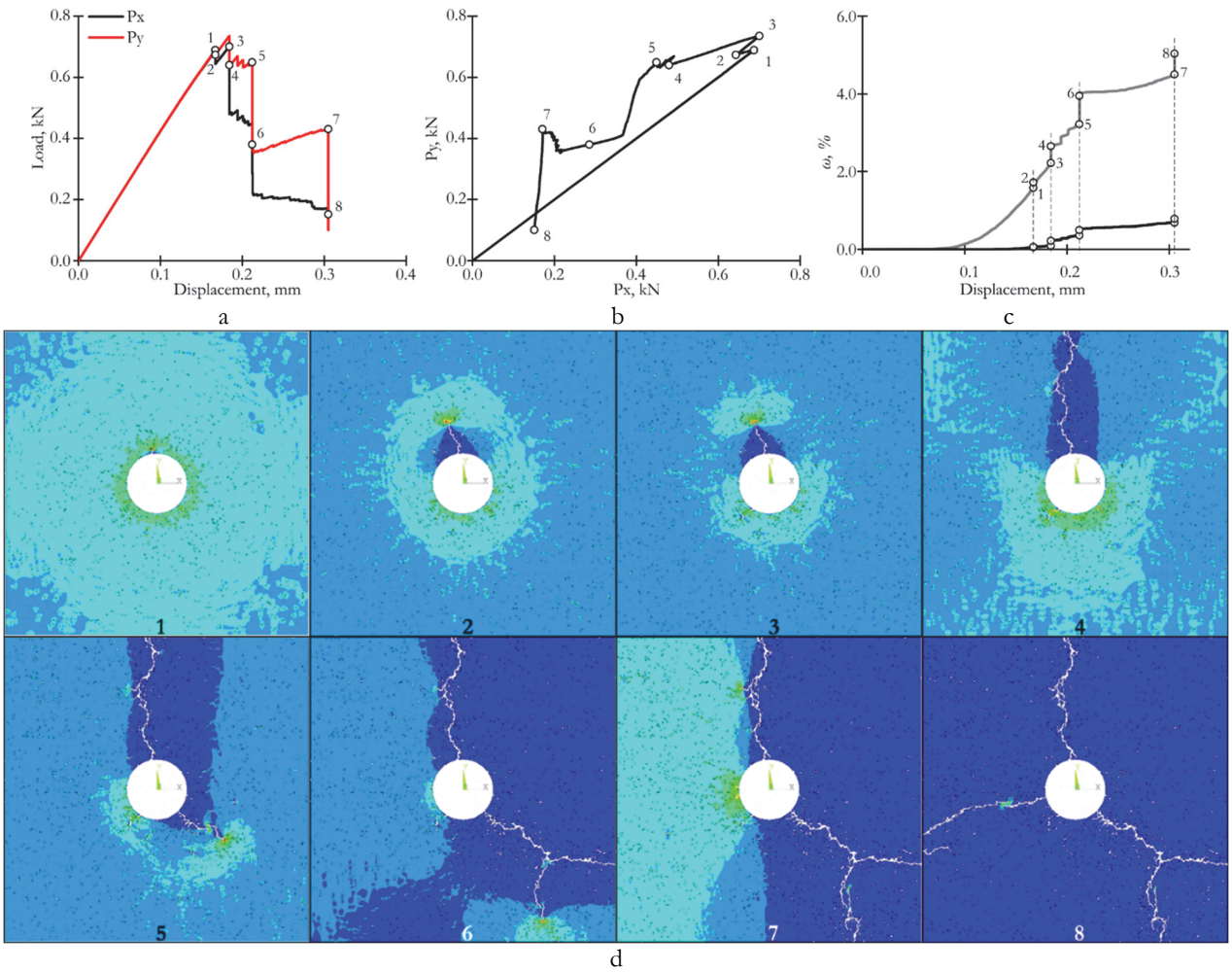

Figure 8: The calculated loading diagrams, states 1–8 are shown on the dependence $P_y(U_y)$ (a), the dependence of P_y on P_x (b), the diagrams of the growth of the relative number of damaged (gray line) and completely fractured (black line) elements (c), the kinetics of the damaging process (d) for CV=0.5 under proportional loading with U_x=U_y.

Consideration of the influence of variation coefficient of strength properties and loading mode on the body type at the moment of calculation completion. The results are shown in Tab. 2 (horizontal images correspond to one generation of ultimate strength limits), white indicates intact areas, gray indicates damaged areas, blue indicates areas with completely lost bearing capacity. It was noted that for cases of uniaxial loading (modes A, E), the macrodefect is oriented across the loading axis, however, for modes of proportional loading with a twofold difference in displacements (modes B, D), the orientation of the macrodefect almost does not change, in some cases the branching of cracks increases. For proportional loading of type C, an increase in macrodefect in arbitrary directions is observed, which is explained by the uniformity of the distribution of the first principal stresses along the contour of the stress concentrator. It is noted that, during the transition from the biaxial loading mode to the uniaxial, damage of individual finite elements in slightly loaded zones (above and below the concentrator for modes E, D, to the right and left of the concentrator for modes A, B) is significantly reduced. For cases CV=0.0 and CV=0.1, there are practically no individual damaged or deactivated finite elements, which corresponds to the localized type of damage accumulation. At CV=0.2, the number of such elements increases, they are concentrated near the concentrator, however, the type of damage accumulation is also closer to the localized than to the mixed. As the CV value increases further, the number of dispersed damaged and deactivated subregions increases, their distribution begins to affect the direction of development of macrodefect, therefore, a mixed type of damage accumulation is realized.

CV	Loading mode				
	A	B	C	D	E
0.0	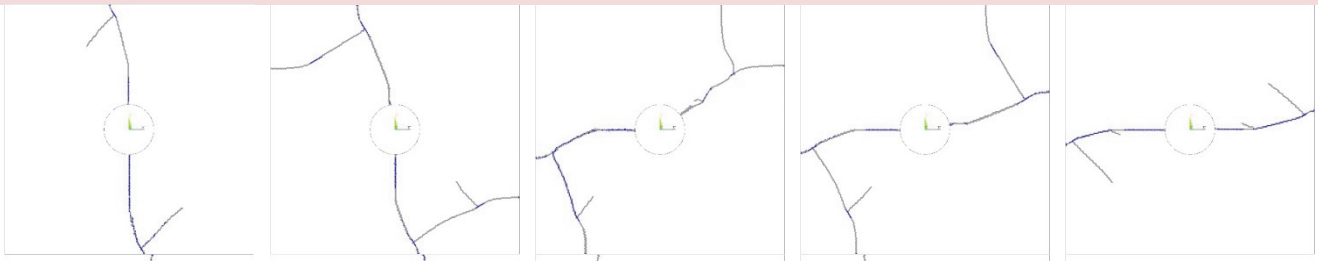				
0.1	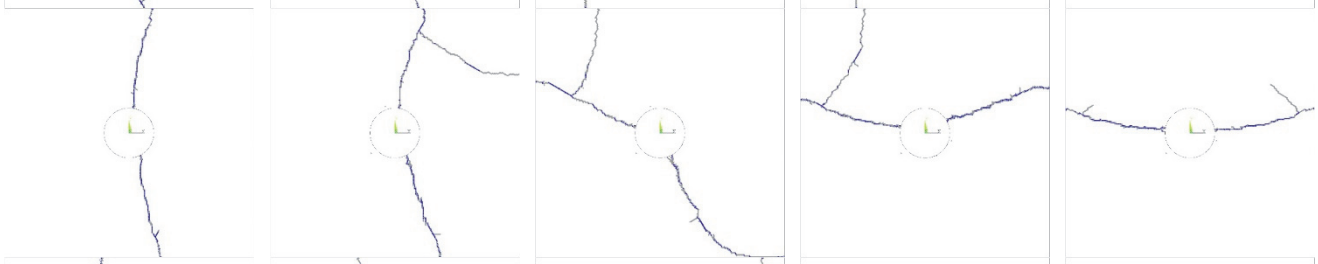				
0.2	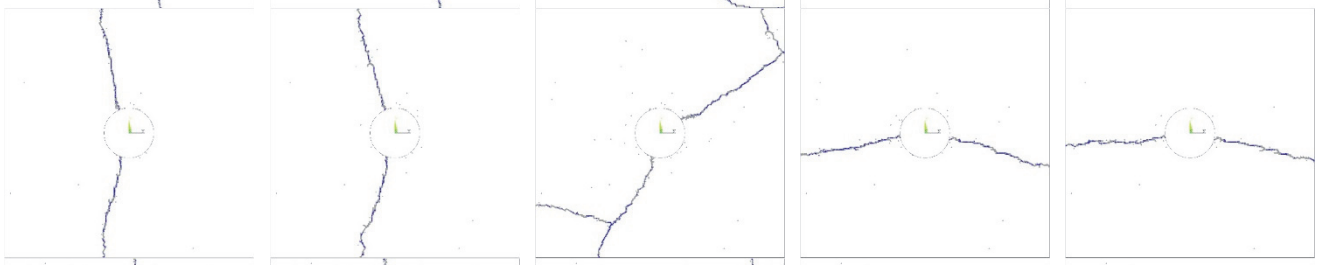				
0.3	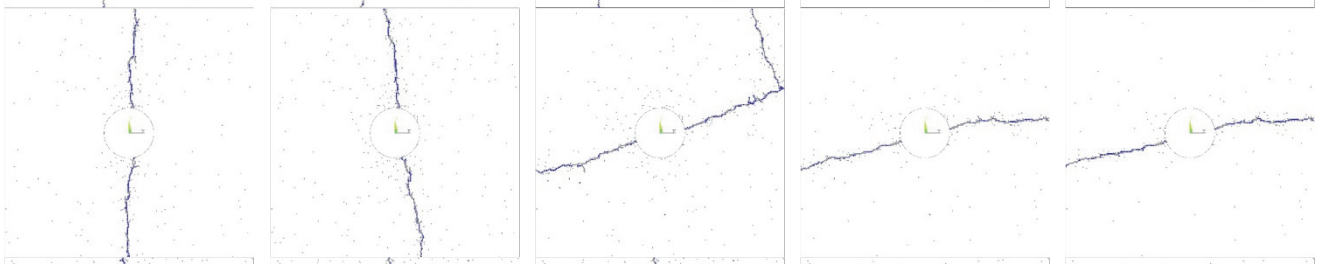				
0.4	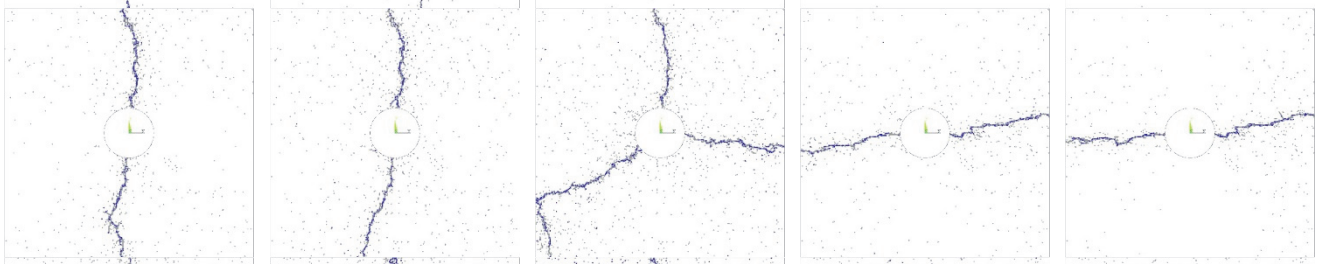				
0.5	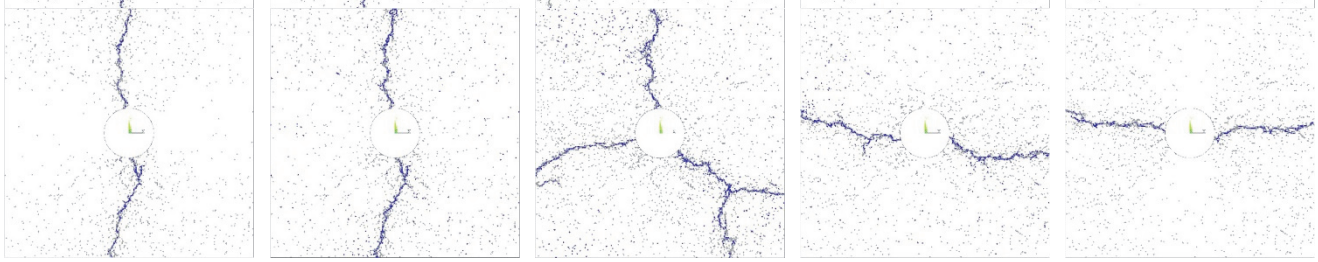				

Table 2: The images of the plate with different coefficients of variation of strength properties for the various loading modes (white color – undamaged zones, grey color – partial damage, blue color – complete fracture).

Based on the obtained results, it was concluded that it is advisable to use the developed model, which considers the appearance of anisotropy with a partial loss of bearing capacity, for modeling the fracture processes of elastic-brittle bodies with randomly distributed strength properties under biaxial loading. For cases of biaxial loading, the effect of a monotonous

decrease in the bearing capacity of the body with an increase in the variation coefficient of strength properties distribution, previously studied in [8], using a uniform distribution of the ultimate strength of structural elements, was confirmed. It has been found that when the elastic-brittle body is proportionally loaded, its bearing capacity is increased in comparison with uniaxial loading. This feature is associated with a decrease in the concentration of stresses at the hole of the contour during the transition from uniaxial loading to proportional loading at $U_x=U_y$. The disproportionality of the $P_y(P_x)$ dependence, associated with the formation of macrodefects that change the cross section of the body in each of the two directions, was revealed. Various types of damage accumulation have been confirmed [7]: localized at $CV\leq0.2$ and mixed at $CV\geq0.3$. The absence of a dispersed type of damage accumulation at high dispersion values of the strength distribution is due to the use of a three-parameter Weibull distribution law and the absence of elements with low strength (which may appear when using a uniform distribution or a two-parameter Weibull distribution). The obtained data on the kinetics of damage accumulation in combination with the loading diagrams should be used for qualitative assessment of the degree of distribution of strength properties in the analysis of experimental data and fractures of samples made of brittle materials. Further use of the developed model for the analysis of fracture processes under disproportionate loading modes is of interest.

Next, the applicability of the previously developed approach to predicting the type of damage accumulation based on the solution of boundary value problems of the elasticity theory will be analyzed.

Applicability of the approach to the assessment of the fracture process' kinetics, based on the analysis of solutions to boundary value problems of elasticity theory

In work [7], the authors developed an approach that consists in assessing the implemented type of damage accumulation based on the analysis of solutions to the boundary value problems of the theory of elasticity. To carry out this assessment, it was proposed to calculate the parameter λ - the average distance from the top of the elliptical hole (in the previous work, a boundary defect was considered) to the centers of mass of the most overloaded elements (in which overload factors exceed the 50% of the maximum value) and the parameter η - the number of the most overloaded elements. Since the problem considers biaxial loading and the central stress concentrator, the parameter λ is calculated as the average distance from the center of the hole to the centers of the most overloaded elements (accordingly, the parameter λ cannot be less than 10 mm - the radius of the hole). This approach will be more versatile for use in various tasks.

Fig. 9a shows body images for different CV values under loading mode C. Red color indicates the most loaded elements; blue – the least loaded elements (overload factors are less than 30% of the maximum value in the body). Figs. 9b, 9c show diagrams of average (by 5 generation of ultimate strength) values of parameters λ and η versus variation coefficient of strength properties CV. The results demonstrate that in the absence of variations in ultimate strength, the area of overloaded elements is formed by a single zone, there are no underloaded elements. With a small variation in mechanical properties (CV=0.1), the number of overloaded elements is significantly reduced, but they are still localized near the contour of the stress concentrator, which explains a significant decrease in the value of η, as well as a decrease in the value of λ to about 15 mm. A further increase in CV to 0.2 led to a further decrease in the number of overloaded elements, however, they began to appear in the body volume far from the stress concentrator, which is associated with the appearance of FE with a tensile strength close to the minimum possible value for this distribution (4.2 MPa). With CV=0.3, the most overloaded FEs are displaced from the hole and their number increases slightly, however, a further increase in the CV value almost does not lead to qualitative and quantitative changes. This is due to the implementation of a mixed type of damage accumulation at $CV\geq0.3$. Therefore, it can be concluded that for proportional loading modes, the indicator of the transition from a localized type of damage accumulation to a dispersed type is the output of diagrams $\lambda(CV)$ and $\eta(CV)$ to the horizontal sections after the decrease in these values at low values of the dispersion of elements' strength properties.

On the basis of the obtained results, it was concluded that it is advisable to apply the developed approach to assessing the type of damage accumulation, based on the analysis of solutions to the boundary value problems of the elasticity theory for a body with randomly distributed mechanical properties. It should be noted that the dependences $\lambda(CV)$ and $\eta(CV)$ are different when using various laws of distribution of strength properties [7]. This feature should be considered when applying the developed approach.

Thus, using the methodology developed in [5-7], this study expands the understanding of the processes of deformation and failure of elastic-brittle bodies with stress concentrators under biaxial loading modes. The disadvantages of the previous work, related to the reduction of all stiffness properties of finite elements when the failure criterion is met, were taken into account: it was proposed to consider the partial loss of bearing capacity and anisotropy, arising from the preservation of resistance in one of the directions. In addition, in order to study the heterogeneity of the distribution of structural elements' strength properties, a three-parameter Weibull distribution law was used, which is better suited for describing the properties of real materials. The improved methodology and algorithms for the modeling of fracture processes developed on its basis

can be successfully applied to studying the patterns of deformation and damage of various structurally inhomogeneous materials (ceramics, polymer composites, etc.).

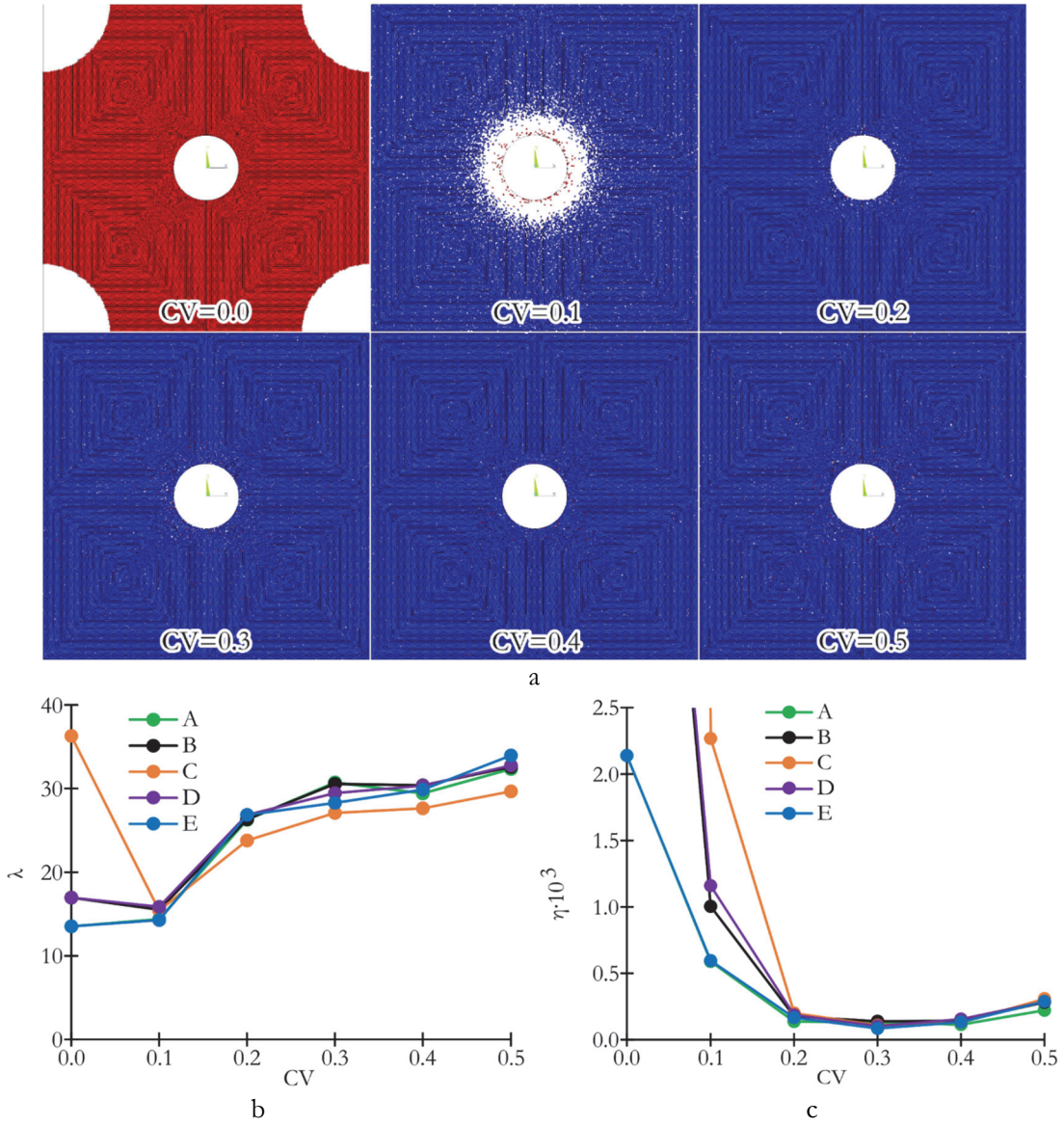

Figure 9: Images of the body (loading mode C) with overloaded (red color) and less loaded (blue color) FEs (a); average distance from the stress concentrator center to the centers of overloaded FEs (b); average number of overloaded FEs (c)

.

Conclusions

In this work, as part of the use of the finite element method, the methodology for modeling the processes of deformation and failure of bodies made of elastic-brittle materials has been improved, based on the consideration of anisotropy, arising from a partial loss of bearing capacity, and the statistical distribution of the strength properties of structural elements. The main results of the study are:

- Statement of the boundary value problem of deformation and failure of a solid body, taking into account partial loss of bearing capacity and non-uniformity of distribution of material properties has been proposed; algorithms for solving the stated boundary value problem has been developed. The feasibility of application of the improved methodology has been demonstrated.
- Influence of statistical distribution of ultimate strength on deformation and failure processes under conditions of various modes of biaxial loading has been studied. The effect of reduction of body's bearing capacity with an increase in the variation

coefficient of the distribution of strength properties has been confirmed. Body's bearing capacity is increased under conditions of uniform biaxial loading.

- The kinetics of damage accumulation processes has been studied, the effect of the loading mode on the orientation of the macrodefect has been considered. As part of the usage of the three-parameter Weibull distribution law, the implementation of the localized and mixed types of damage accumulation has been confirmed.
- The applicability of the previously developed approach to assessing the type of damage accumulation, based on the analysis of numerical solutions of boundary value problems of elasticity theory, has been evaluated. The feasibility of using this approach for various laws of distribution of strength properties and loading modes has been demonstrated.

Further studies will be aimed at improving the developed methodology for performing numerical modeling of the processes of deformation and failure of bodies made of anisotropic materials under various loading modes, as well as at comparing the results of numerical solutions of boundary value problems with the experimental data.

ACKNOWLEDGEMENTS

This research was funded by Ministry of science and higher education of the Russian Federation (Project № FSNM-2024-0013).

REFERENCES

[1] Vildeman, V.E., Sokolkin, Y.V. and Tashkinov, A.A. (1995). Boundary-value problem in the mechanics of the deformation and failure of damaged bodies with yielded zones, J. Appl. Mech. Tech. Phys., 36, pp. 903–911. DOI: https://doi.org/10.1007/BF02369389.

[2] Brocks, W. and Schwalbe, K.-H. (2016). Experimental and Numerical Fracture Mechanics—An Individually Dyed History, London, Springer. DOI: https://doi.org/10.1007/978-3-319-21467-2_2.

[3] Carpinteri, A. Nonlinear Crack Models for Nonmetallic Materials. (1999).Nonlinear Crack Models for Nonmetallic Materials, Dordrecht, Springer. DOI: https://doi.org/10.1007/978-94-011-4700-2.

[4] Markides, C. and Kourkoulis, S. K. (2023). Revisiting classical concepts of Linear Elastic Fracture Mechanics - Part I: The closing 'mathematical' crack in an infinite plate and the respective Stress Intensity Factors. Fracture and Structural Integrity, 17(66), pp. 233–260. DOI: https://doi.org/10.3221/IGF-ESIS.66.15.

[5] Wildemann, V.E., Feklistova, E.V., Mugatarov, A.I., Mullahmetov, M.N. and Kuchukov, A.M. (2023). Aspects of numerical simulation of failure of elastic-brittle solids, Comput. Contin. Mech., 16(4), pp. 420–429. DOI: https://doi.org/10.7242/1999-6691/2023.16.4.35.

[6] Feklistova E., Mugatarov A., Wildemann V., Agishev, A. (2024). Fracture processes numerical modeling of elastic-brittle bodies with statistically distributed subregions strength values. Fracture and Structural Integrity, 18(68), pp. 425–439. DOI: https://doi.org/10.3221/IGF-ESIS.68.22.

[7] Feklistova, E., Mugatarov, A. and Wildemann, V. (2024). Numerical study of the influence of the parameters of statistical distribution of the structural elements' ultimate strength on deformable bodies' fracture processes. Fracture and Structural Integrity, 18(70), pp. 105–120. DOI: https://doi.org/10.3221/IGF-ESIS.70.06.

[8] Feklistova E.V., Mugatarov, A.I. and Wildemann, V.E. (2024). Simulation of fracture in deformable bodies with stress concentrators taking into account the statistical distribution of ultimate strength in structural elements. PNRPU Mechanics Bulletin, 4, pp. 70-83. DOI: https://doi.org/10.15593/perm.mech/2024.4.07.

[9] Vishwanatha, H.S., Muralidhara, S. and Raghu Prasad, B.K. (2025). Size Effect in Concrete Beams: A Numerical Investigation Based on the Size Effect Law. Fracture and Structural Integrity, 19(73), 23–40. DOI: https://doi.org/10.3221/IGF-ESIS.73.03.

[10] Novembre, E., Airoldi, A., Riva, M. and Caporale, A.M. (2024). A macroscale damage model for the tensile and bending failure of C/C-SiC structural laminates, Journal of the European Ceramic Society, 44(13), pp. 7490–7503. DOI: https://doi.org/10.1016/j.jeurceramsoc.2024.05.072

[11] Picu, R.C. and Jin, S. (2023). Toughness of network materials: Structural parameters controlling damage accumulation, 172, 105176. DOI: https://doi.org/10.1016/j.jmps.2022.105176

[12] Airoldi, A., Mirani, C. and Principito, L. (2020). A bi-phasic modelling approach for interlaminar and intralaminar damage in the matrix of composite laminates, Composite Structures, 234, 111747.

DOI: https://doi.org/10.1016/j.compstruct.2019.111747.
[13] Pabbu, K.M., Muthu, N. and Pallicity, T.D. (2025). Polynomial-based damage model with EAS approach to model isotropic continuum damage in hyperelastic materials, Finite Elements in Analysis and Design, 247, 104350. DOI: https://doi.org/10.1016/j.finel.2025.104350.
[14] Rui J., Li, Z.-H., Wang, C.-H. and Zhang, Ya-S. (2024). Structural overall damage index based on structural strain energy, Structures, 60, 105829. DOI: https://doi.org/10.1016/j.istruc.2023.105829.
[15] Liu, Y.-Yi, Chen, J.-B. and Li, J. (2024). The modified mesoscopic stochastic fracture model incorporating the random field of Young's modulus for the uniaxial constitutive law of concrete, Probabilistic Eng. Mech., 75, 103585. DOI: https://doi.org/10.1016/j.probengmech.2024.103585.
[16] Hai, L. and Lyu, M.-Z. (2023). Modeling tensile failure of concrete considering multivariate correlated random fields of material parameters, Probabilistic Eng. Mech., 74, 103529. DOI: https://doi.org/10.1016/j.probengmech.2023.103529.
[17] Chen, X. and Li, J. (2023). An extended two-scale random field model for stochastic response analysis and its application to RC Short-leg shear wall structure, Probabilistic Eng. Mech., 74, 103508. DOI: https://doi.org/10.1016/j.probengmech.2023.103508.
[18] Zheng, T., Guo, L., Ding, J. and Li, Z. (2022). An innovative micromechanics-based multiscale damage model of 3D woven composites incorporating probabilistic fiber strength distribution, Compos. Struct., 287, 115345. DOI: https://doi.org/10.1016/j.compstruct.2022.115345.
[19] Khechai, A. and Mohite, P. (2019). Optimum design of perforated symmetric laminates using evolutionary algorithm. J. Compos. Mater., 53 , pp. 3281–3305. DOI: https://doi.org/10.1177/0021998318815324.
[20] Khechai, A., Layachi, M., Belarbi, M.-O. and Gohery, S. (2025). An extended Greszczuk's analytical method for stress analysis of unsymmetrical laminated composite plates with a circular hole under axial, biaxial, and shear loads. Structures, 71, 108169. DOI: https://doi.org/10.1016/j.istruc.2024.108169.
[21] Jagannathana, N., Gururaja, S., and Manjunatha, C.M. (2019). Matrix cracking in polymer matrix composites under bi-axial loading, Procedia Structural Integrity, 14, pp. 864–871. DOI: https://doi.org/10.1016/j.prostr.2019.07.065.
[22] Y., Luo and Hu, H. (2009). Mechanical properties of PVC coated bi-axial warp knitted fabric with and without initial cracks under multi-axial tensile loads, Composite Structures, 89(4), pp. 536–542. DOI: https://doi.org/10.1016/j.compstruct.2008.11.007.
[23] Strungar, E., Lobanov, D., Chebotareva, E. and Kochneva, Y. (2024). Mechanical behavior of fiber-glass plastic with hole pattern using digital image correlation and acoustic emission methods. Fracture and Structural Integrity, 18(68), pp. 63–76. DOI: https://doi.org/10.3221/IGF-ESIS.68.04.
[24] Khechai, A., Tati, A., Guettala, A. and Mohite, P.M. (2018). A general solution for stress resultants around a circular cutout in laminate plates under different in-plane loadings: analytical and experimental investigations, Arch. Appl. Mech., 88, pp. 1187–1208. DOI: https://doi.org/10.1007/s00419-018-1366-x.
[25] Ma, C., J., Xu, Liu, Z. and Lv, Z. (2023). Study on mechanical properties and failure mode of single-fissure sandstone discs under bi-directional linear loading, Theoretical and Applied Fracture Mechanics, 128, 104164. DOI: https://doi.org/10.1016/j.tafmec.2023.104164.